Desalination and Water Treatment
www.deswater.com

doi: 10.5004/dwt.2023.29601

295 (2023) 205–216
May

Enhanced biosorption of hexavalent chromium ions from aqueous solution onto *Ziziphus jujube* seeds as ecofriendly biosorbent – equilibrium and kinetic studies

T. Hariharan[a,*], R. Gokulan[b,*], N. Al-Zaqri[c,*], I. Warad[d,e]

[a]*Department of Chemical Engineering, Mohamed Sathak Engineering College, Kilakarai 623806, Tamil Nadu, India, email: hariharanthangappan@gmail.com*
[b]*Department of Civil Engineering, Vallurupalli Nageswara Rao Vignana Jyothi Institute of Engineering and Technology, Hyderabad 500 090, Telangana, India, email: gokulravi4455@gmail.com*
[c]*Department of Chemistry, College of Science, King Saud University, P.O. Box: 2455, Riyadh 11451, Saudi Arabia, email: nalzaqri@ksu.edu.sa*
[d]*Department of Chemistry, AN-Najah National University, P.O. Box: 7, Nablus, Palestinian Autority, email: i.kh.warad@gmail.com*
[e]*Research Centre, Manchester Salt and Catalysis, Unit C, 88-90 Chorlton Rd., M154AN Manchester, United Kingdom, email: i.kh.warad@gmail.com*

Received 26 December 2022; Accepted 30 April 2023

ABSTRACT

Batch adsorption of chromium metal ions from the aqueous solutions was studied using activated biochar material from *Ziziphus jujube* seed powder. Using the chemical synthesis technique, the adsorbent material was produced and activated by concentrated sulfuric acid. The characterization of the adsorbent material produced was performed through scanning electron microscopy and Fourier-transform infrared spectroscopy analyses, while the size of the pores was determined using Brunauer–Emmett–Teller isotherm analysis. Batch experiments were used to determine the best parameters for pH, contact duration, dose, ion concentration, temperature, and particle size. Adsorption isotherm studies were performed to verify the adsorption process, and kinetic experiments were performed to determine the nature of chromium ion absorption by the adsorbent. Thermodynamic tests confirmed that the adsorbent's metal absorption is endothermic. 93.27% of chromium ions were desorbed from the wasted adsorbent using 0.3 N HCl. Using activated *Ziziphus jujube* biochar as an adsorbent, around 99.27% of the chromium ions were adsorbed from the generated synthetic solution.

Keywords: Biosorption; *Ziziphus jujube* powder; Chromium ions; Kinetic studies; Equilibrium studies

1. Introduction

Chromium is one of the important elements for manufacturing ceramic metals, electroplating, dyes, paints, and leather. It is soluble in water at 20°C, and the melting point of chromium is 1907 +/– 10°C. The chromium metal ions play an important role in all kinds of the industrial manufacturing process [1]. Due to the rapid population growth and industrial expansion, there is an urgent need for all kinds of industrial-oriented products. At the same time, the surrounding environment gets highly contaminated due to various kinds of industrial activities. Chromium is a normal metal ion available everywhere on the earth's surface. While processing the chromium for getting the products, the oxidate state of chromium ions gets increased or decreased, and it becomes a heavy metal ion [2]. Heavy metals are very toxic compared to normal metal ions, creating harmful effects on the surrounding environment even in very low concentrations.

* Corresponding authors.

Chromium ions were converted into trivalent (Cr^{3+}) and hexavalent (Cr^{6+}) states during the processing of industrial products. These states of chromium ions are usually called chromium heavy metal ions. The hexavalent chromium ions (Cr^{6+}) are highly toxic, creating cancer and respiratory problems for humans while consuming more than the acceptable limit of 0.05 mg/L. A large volume of effluent with very high concentrations of hexavalent chromium ions was discharged into natural water bodies as a result of the processing of industrial goods such as tanning and electroplating [3]. These ions are non-degradable and, mixed with clean water, create toxic environmental effects. Hence it is necessary to reduce the concentration of heavy metal ions from the industrial effluent. The physical and chemical methods adopted in normal effluent treatment plants (ETPs) are unsuitable for treating water from metal ion concentrations. Various treatment methodologies such as filtration, precipitation, ion exchange, membrane adsorption were used to remove these pollutants from the aqueous medium. These methods have disadvantages like secondary sludge generation, high reagent requirement, high investment, maintenance cost etc. Among these methods, adsorption was used most widely to reduce/remove the concentration of toxic pollutants from the aqueous medium. It is one of the simplest processes and requires very low investment and maintenance costs [4]. The process of accumulating pollutants on the adsorbent's surface is called adsorption. For receiving the pollutants from the aqueous solutions, a substance was used, and it is called an adsorbent working under the van der Waal's force [5].

Biochar is a material produced from naturally available waste biomass. In recent years biochar is considered as one of the promising methods for pollution abatement. It plays an important role in waste reduction as well as low-cost material for pollution removal. Biochar was extensively used for soil remediation in the past and in recent years it had a widespread application in the area of wastewater treatment, heavy metals removal, construction industries, greenhouse gas reduction, and carbon sequestration. Physical and chemical characteristics of the biochar play an especially important role in the pollution abatement. Some of the important properties of the biochar are particle size, density, moisture content, porosity, and chemical composition. The characteristics of biochar are determined by both the type of feedstock and the production methods employed. In general, dry feedstock is preferred over wet feedstock, as the latter has a moisture content of over 30%, which can increase the initial cost for pretreatment. Pyrolysis, gasification, torrefaction, and hydrothermal carbonization are some of the thermo-chemical methods that can be used for biochar production. These methods can be categorized into three main types: slow pyrolysis, fast pyrolysis, and flash pyrolysis. Of all these methods slow pyrolysis was considered as one of the best methods. The biochar produced from slow pyrolysis will have high surface area, pore size and pore volume. The formation of micropores is very high that could enhance the removal efficiency.

One of the most challenging tasks is identifying the sorbent, and all these adsorbent materials assure the adsorption process's performance. Various compostable and decomposable materials were used, such as tree bark and leaves, shells, fruit peels and seeds, etc., to remove the toxic pollutants from the aqueous medium. The present study focused on utilizing activated carbon derived from *Ziziphus jujube* seeds as a biosorbent for removing hexavalent chromium ions from aqueous solutions. Using adsorption isotherm and kinetics the process of metal ion uptake by the adsorbent was evaluated. Table 1 summarizes the numerous studies that have been undertaken utilizing *Ziziphus jujube* products as an adsorbent material.

2. Materials used and methods

2.1. Stock and biochar adsorbent preparation

Potassium dichromate powder (100 mg) was mixed with 1 L of distilled water, and the synthetic solution was prepared with a concentration of 100 mg/L. Adjusting the concentrations was accomplished by combining the required amount of distilled water with potassium dichromate powder. The adsorbent material was prepared by crushing the *Ziziphus jujube* seeds using a mechanical crusher after 24 h of sun drying. The powdered sample was then placed in a muffle furnace and heated to 300°C to transform it into charcoal. The charcoal powder was removed from the furnace and washed with strong sulfuric acid for chemical activation (H_2SO_4). To remove the water content, activated charcoal *Ziziphus jujube* seeds powder was roasted for 8 h at 100°C. The sample was taken out of the oven and will be used in future studies.

2.2. Adsorbent characteristics studies

The surface area of the generated biochar *Ziziphus jujube* adsorbent was initially evaluated using nitrogen adsorption and desorption at –196°C. Eq. (1) was used

Table 1
Adsorption of various pollutants using *Ziziphus jujube* biosorbent

S. No.	Name of the metal ion/dye	Adsorption efficiency	Initial concentration of pollutants	Optimum pH	Ideal dose	Contact time	References
1.	Cr^{6+}	99.27%	0.02 g/L	2.0	600 mg/L	1 h 30 min	In this study
2.	Cd^{2+}	50 mg/g	0.05 g/L	2.0	1600 mg/L	0.4 h	[6]
3.	Cr^{6+}	61.92%	0.1 g/L	2.0	1000 mg/L	2 h	[7]
4.	Cd^{2+} and Pb^{2+}	16.47 and 20.98 mg/g	60 mg/L	3.0	2 g/L	2 h	[8]
5.	As^{2+}	79.3%	40 mg/L	5.0	1.5 mg/L	20 h	[9]

to determine the micro and mesopores of the biosorbent material. Prior to obtaining the level of pore sizes, the biosorbent material was heated to 300°C to remove any gas molecules and was subjected to a vacuum.

$$S_m = S_{\text{BET}} - S_u \tag{1}$$

The average sizes of the micro and mesopores present in the *Ziziphus jujube* biosorbent were denoted as S_m and S_u, respectively, while S_{BET} represented the average surface area calculated using Brunauer–Emmett–Teller (BET) analysis. The pore volume (VT) and liquid nitrogen acquired for BET analysis were evaluated at a relative pressure of P/P_o~0.99 [10]. Eq. (2) was employed to calculate the volume of the micro and mesopores.

$$V_m = V_T - V_u \tag{2}$$

The average pore diameter (D_p) was obtained using the Barrett–Joyner–Halenda (BJH) model represented in Eq. (3).

$$D_P = \frac{4V_T}{S_{\text{BET}}} \tag{3}$$

Fourier-transform infrared spectroscopy (FTIR) studies evaluated the functional group availability in the prepared adsorbent by taking the initial concentration of Cr^{6+} ions in the synthetic solution 20 mg/L, pH of the solution 5.0 and 1 g of *Ziziphus jujube* biosorbent used. To avoid floc formation and ensure appropriate mixing, the solution was shaken for 3 h at a speed of 200 rpm in a rotary shaker. Following that, the solution was allowed to settle for up to 10 min before being suspended for the various experimental processes. The bandwidth of 400–4,000 cm^{-1} was fixed in FTIR studies with a range interval of 4 cm^{-1} and 20 scans were done for functional group checking. The energy-dispersive X-ray spectroscopy (EDX) analysis equipped with scanning electron microscopy (SEM) instrument was performed to check the surface fractions and flaws.

2.3. Batch studies

The study investigated the effects of varying adsorption parameters, such as pH, ion concentration, contact time, adsorbent dosage, and temperature, on the batch mode adsorption process. The pH of the solution was adjusted from 2.0 to 7.0 to determine the optimal value for maximum metal ion removal. The batch mode adsorption study was conducted by adjusting the biosorbent dosage level from 0.1 to 1.0 g/L and varying the chromium concentration in the aqueous solution from 20 to 100 mg/L at 30°C within a time interval of 30–180 min. The metal ion adsorption process was represented by the mass balance system approach, as shown in Eq. (4).

$$q_t = \frac{V}{m}\left(C_0 - C_t\right) \tag{4}$$

The concentration of aqueous medium was represented by C_t and amount of heavy metals uptake by the biochar material was signified by q_t. Total amount of chromium ions adsorbed on the adsorbent's surface was evaluated using the AAS (AA6300) spectrophotometry analyzer. To obtain the concurrent value, each analysis was done twice. Eq. (5) depicts the mass balance system of the metal ion adsorption process.

$$\%\text{Removal} = \left[\frac{C_o - C_e}{C_e}\right] \times 100 \tag{5}$$

The initial and final concentration of synthetic solution with hexavalent chromium ions was represented by C_0 and C_e, respectively.

2.4. Isotherm studies

Mathematical equations and certain assumptions evaluated the performance of targeted metal ion uptake by the biosorbent materials. These assumptions and mathematical equations are usually called isotherm studies, which check the adsorbate transmission from the solution phase to the adsorbent phase under a controlled temperature [11]. The isotherm investigations listed below are often performed to examine the adsorption process utilizing the adsorbent material.

2.4.1. Langmuir isotherm

During the equilibrium conditions, the behavior and concentrations of the fluid and solid phases were evaluated in relation to the solid and gas phases, as determined by Langmuir isotherm studies. Because of chemical reactions, the process of adsorption happened, which is the basic assumption of the Langmuir isotherm study. Furthermore, the adsorbent absorbs metal ions in a homogeneous monolayer adsorption process [12]. Based on these assumptions, the Langmuir isotherm was derived and represented in Eq. (6) at a given temperature of 30°C.

$$\frac{C_e}{q_e} = \frac{1}{K.q_{\max}} + \frac{C_e}{q_{\max}} \tag{6}$$

where C_e denotes the concentration of chromium metal ion-containing solution, q_e denotes the adsorbed quantity of ions per g and $q_{\max}$ and K denotes the Langmuir model constants for intensity and capacity.

2.4.2. Freundlich isotherm

At 30°C of constant temperature the Freundlich isotherm studies were conducted to check the multilayer adsorption with heterogeneous nature in batch mode. The variations in metal ion adsorption from the adsorbed gas using a mass of activated *Ziziphus jujube* powder in unit mass were described by this study at a given temperature [13]. The Freundlich isotherm model was developed using linear Eq. (7) at a given temperature of 30°C.

$$\frac{1}{q_e} = \frac{1}{K_f} + \frac{1}{n}C_e \tag{7}$$

where q_e represents the quantity of chromium ions adsorbed by *Ziziphus jujube* adsorbent, capacity and energy of the

adsorption process is represented by n and K_f, and C_e represents chromium ion concentration in the synthetic solutions at equilibrium.

2.4.3. Sips isotherm

The Sips model isotherm study was used to predict the adsorption process in very low concentrations. To study the homogenous sites in the adsorbent material, this sort of isotherm model was created from Langmuir and Freundlich isotherm investigations. The Sips model isotherm assumes a monolayer adsorption process and disregards the concentration of chromium ion solutions [14]. Eq. (8) can be expressed the linear study of Sips isotherm model at 30°C.

$$\frac{1}{q_e} = \frac{1}{Q_{\max} K_S} \left(\frac{1}{C_e} \right)^{\frac{1}{n}} + \frac{1}{Q_{\max}} \tag{8}$$

where $Q_{\max}$ and K_s represent equilibrium and adsorption capacity, respectively, whereas n denotes heterogeneity.

2.4.4. Redlich – Peterson isotherm

This study utilizes a mix of the Langmuir and Freundlich models, which is also the case for the Sips isotherm study. Instead of the monolayer, this Redlich–Peterson isotherm model analyses the multilayer adsorption process with heterogeneous nature. The adsorption mechanism between biosorbent and targeted metal ion is unique, and the multilayer adsorption process has been considered [15]. Eq. (9) can be expressed the linear model of Redlich–Peterson isotherm model at 30°C.

$$\ln \frac{C_e}{q_e} = \beta \ln C_e - \ln A \tag{9}$$

where β and A represent the exponent value and Redlich–Peterson isotherm constant.

2.5. Kinetic studies

To investigate the solute releases from the synthetic solutions during the process of metal ion uptake, kinetic models were used. The data obtained from the batch studies have been used to evaluate the process of adsorption to the solid interface due to strong and weak forces. The following kinetic studies were performed to check the performance of adsorption process.

2.5.1. Pseudo-first-order kinetics

In between hard and fluid adsorption systems, the strong driving force was developed, and the chromium ion uptake by *Ziziphus jujube* seeds is directly proportional to the capacity of adsorption are the basic assumptions of this kinetic model [16]. Using the linear plots obtained from Eq. (10), the initial and equilibrium concentrations between chromium ion adsorption using *Ziziphus jujube* seeds were evaluated.

$$\frac{dq_e}{dq_t} = k\left(q_e - q_t\right) \tag{10}$$

The chromium ions adsorbed by *Ziziphus jujube* seeds powder was obtained by calculating q_e and q_t values after applying the boundary conditions in Eq. (10) has been converted to Eq. (11).

$$Q_t = Q_e\left(1 - e^{-kt}\right) \tag{11}$$

2.5.2. Pseudo-second-order kinetics

Based on the assumption that the amount of metal ions absorbed by activated *Ziziphus jujube* seeds powder is related to the biosorbent's active site count, the linear plots were derived by referring to Eq. (12).

$$\frac{t}{q} = \frac{1}{h} + \frac{1}{q_e} t \tag{12}$$

The earlier reaction time was determined using the equation $h = kq_e^2$ and the values of k, h and q_e were obtained from the linear plots.

2.5.3. Elovich kinetics

The existence of gas molecules was detected in the *Ziziphus jujube* seeds charcoal adsorbent during the beginning step of the chromium metal ion adsorption process. Based on this condition, the increase in the amount of metal ions adsorbed from the solute is exponentially proportional to the decrease in desorption rate [17,18]. Eq. (13) expresses the Elovich kinetic plot based on the above assumptions.

$$q_t = \frac{\ln a_e b_e}{b_e} + \frac{1}{b_e} \ln t \tag{13}$$

where a_e and b_e are the Elovich model parameters in mg/g and g/mg.

3. Results and discussion

3.1. BET isotherm analysis.

At –196°C the process of adsorption and desorption were conducted and the curve for this study is shown in Fig. 1. Referring to the figure the adsorption follow-up

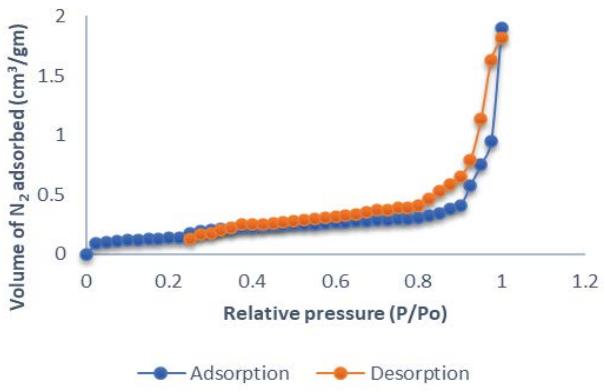

Fig. 1. Adsorption and desorption curve of biosorbent material for Brunauer–Emmett–Teller analysis.

procedure by type II category using two curves. In other words, the first curve shows the presence of micropores, whereas the second depicts the presence of mesopores in the biochar adsorbent [19]. By observing the two curves in the plot, it can be inferred that the *Ziziphus jujube* biosorbent has a significantly high surface area, along with a substantial level of micro and mesopores, which enable it to effectively adsorb pollutants from the source. The obtained area of surface of 468 m^2/g indicates applicability range of their commercial activated carbons. Table 2 represents the various characteristics values of biosorbent obtained from the BET analysis.

3.2. FTIR studies

The presence of functional groups was examined by FTIR studies with the range of 400–4,000 cm^{-1}. Before and after the chemical activation process of *Ziziphus jujube* adsorbent and its functional groups were analyzed by this study. Fig. 2a and b show the availability of various functional groups in both natural and activated biochar adsorbents. Before chemical activation process the charcoal adsorbent has the peak at 1,600 cm^{-1} and it represents the ring vibrations of carbonyl groups. Fig. 2b depicts the highest peak at 2,924 cm^{-1} caused by symmetrical bending of O–H groups. Also, the peak at 1,595 cm^{-1} was developed due to the vibrations of bending by $–CH_2$ groups. At the peak of 3,392 cm^{-1} the alcohol stretching was observed and 1,092 cm^{-1} peak, –COO vibration stretch was identified [20]. The preceding explanation concludes that the activated *Ziziphus jujube* biochar adsorbent has a large number of functional groups for receiving contaminants from aqueous solutions.

3.3. SEM analysis

Fig. 3a and b show activated charcoal biosorbent before and after Cr^{6+} metal ion absorption at 10 and 5 μm working distances, respectively. The adsorbent's surface has multiple active sites and irregular pores before absorbing the metal ions, as shown in first two SEM images. These active sites and pores are critical in absorbing toxic metal ions in the wastewater. The microscopic image acquired after passing the synthetic solution onto the charcoal biosorbent is shown in Fig. 3b. Pollutants accumulated in the active sites and pores, producing a cloud on the adsorbent surface [21]. The pollutants were adsorbed onto the surface of the adsorbent through the micro and mesopores, until the point of saturation was reached. Beyond that, there is no pollutant uptake was observed. The preceding discussion verifies the presence of contaminants on the surface of the adsorbent.

Table 2
Characteristics of *Ziziphus jujube* biochar adsorbent

Type of property	Value obtained
Surface area (BJH), m^2/g	76.983
Pore volume, cc/g	0.116
Pore radius, Å	32.822
Surface area (BET), m^2/g	468
Pore diameter (Avg.), nm	0.0057

EDX analysis was used to assess the targeted metal ion efficiency and its presence.

3.4. EDX analysis

Similar to the SEM analysis, the EDX analysis was performed before and after metal ion adsorption using the biochar adsorbent. EDX pictures of the produced biochar adsorbent before and after chromium ion adsorption are shown in Fig. 4a and b. The surface of the biochar adsorbent contains a variety of chemical and metallic elements, including large amounts of carbon, as well as oxygen, calcium, and other elements. The diffraction image of the metal ion containing solution after reaching the saturation point was captured when it was passed through the biochar adsorbent, as depicted in Fig. 4b. The presence of carbon and oxygen were not the only elements observed on the adsorbent's surface, but also chromium, potassium, and alumina, which confirmed the existence of the desired metal ion [22].

3.5. Impact of pH in chromium removal

The efficiency of adsorption and its changes due to the variations of pH in the synthetic solution was examined by fixing the ion concentration of 20 mg/L and biosorbent dose of 1.0 g/L. The reaction time was fixed at 60 min with decreasing the pH of aqueous solution from 7.0 to 2.0 by adding the pH HNO_3 solution. Around 98.82% of chromium ions were eliminated from the synthetic solution with an optimal pH of 2.0 at 30°C of the solution's temperature. The raise in pH of synthetic solution decreases the adsorption

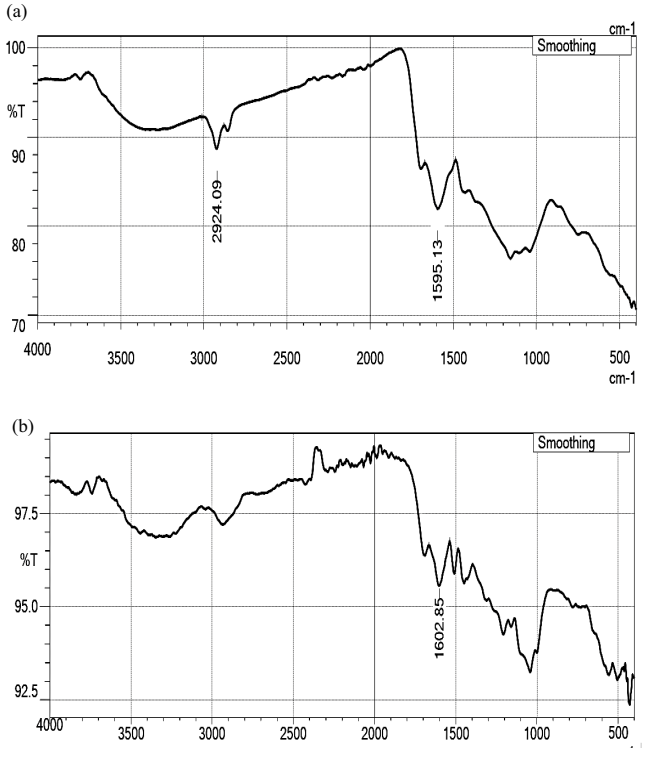

Fig. 2. Fourier-transform infrared spectroscopy stretching peaks of biosorbent before and after metal ion uptake.

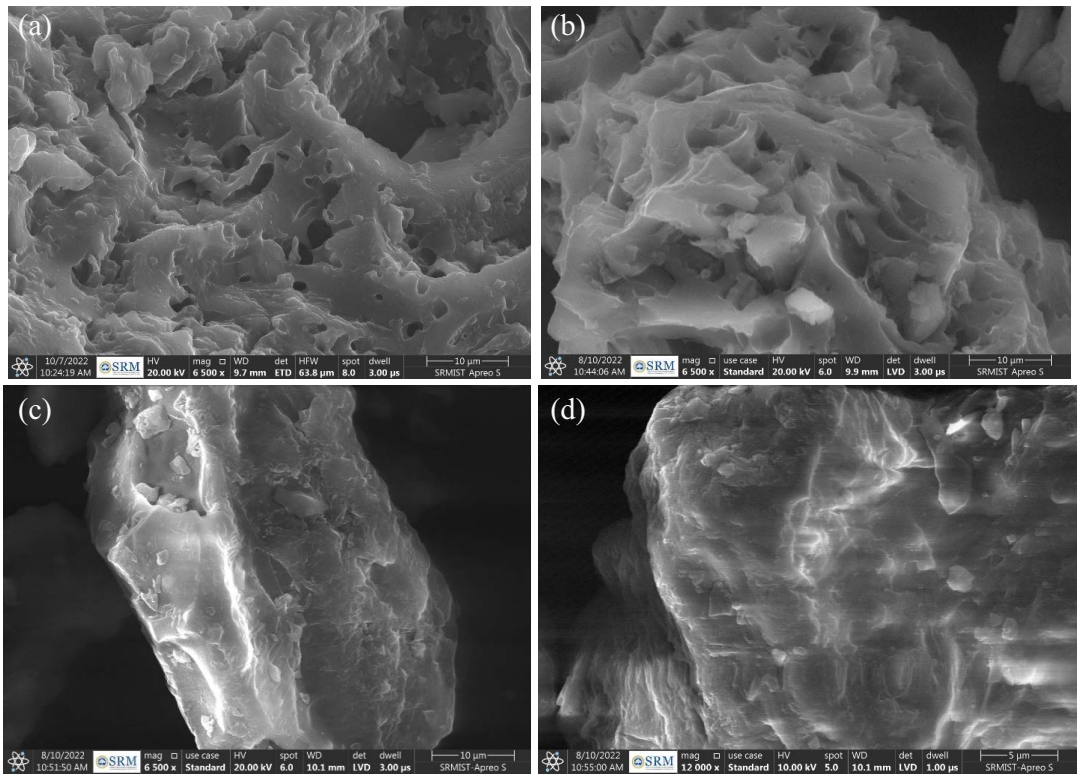

Fig. 3. Scanning electron microscopy images of biosorbent material (a) before and (b) after chromium uptake.

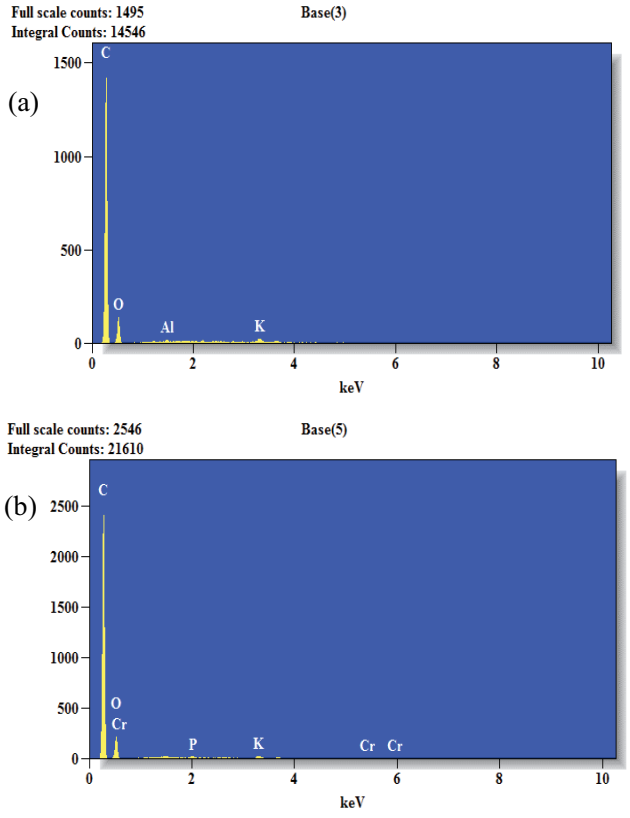

Fig. 4. Energy-dispersive X-ray spectroscopy images of biosorbent (a) before Cr adsorption and (b) after Cr adsorption.

efficiency is seen in Fig. 5a. When the pH is low, that is, when the solution is strongly acidic, positively charged ions play an important role in attracting negatively charged ions and boosting the efficiency rate [23]. An increase in the pH of the solution reduces the amount of adsorption efficiency because of hydroxyl precipitation.

3.6. Impact of biochar dose in chromium removal

The amount of active sites in the adsorbent determines the amount of metal ion removal from the aqueous medium. With optimum pH of 2.0, the biosorbent dose in the synthetic solution was increased from 0.1 to 1.0 g/L and the impact in ion removal efficiency were investigated. At 30 min of reaction time the impact of adsorption efficiency was studied for 20 mg/L ion concentrated synthetic solution. The impact of chromium ion adsorption on the dose of *Ziziphus jujube* seeds at 30°C is depicted in Fig. 5b. As seen in the figure, the rise in adsorbent dose enhanced the adsorption efficiency. Above 0.6 g/L of biosorbent dose, there was a decrease in ion efficiency, indicating the adsorption process's saturation point. Following the saturation stage, all active sites are contaminated, and the number of available vacant sites is severely restricted, lowering adsorption effectiveness. According to the findings, 0.6 g/L of activated biochar *Ziziphus jujube* seeds eliminated 98.37% of the chromium ions from the generated synthetic solution.

3.7. Impact of chromium concentration

Increasing the concentration of solution decreases the adsorption efficiency because of presence of very high ion

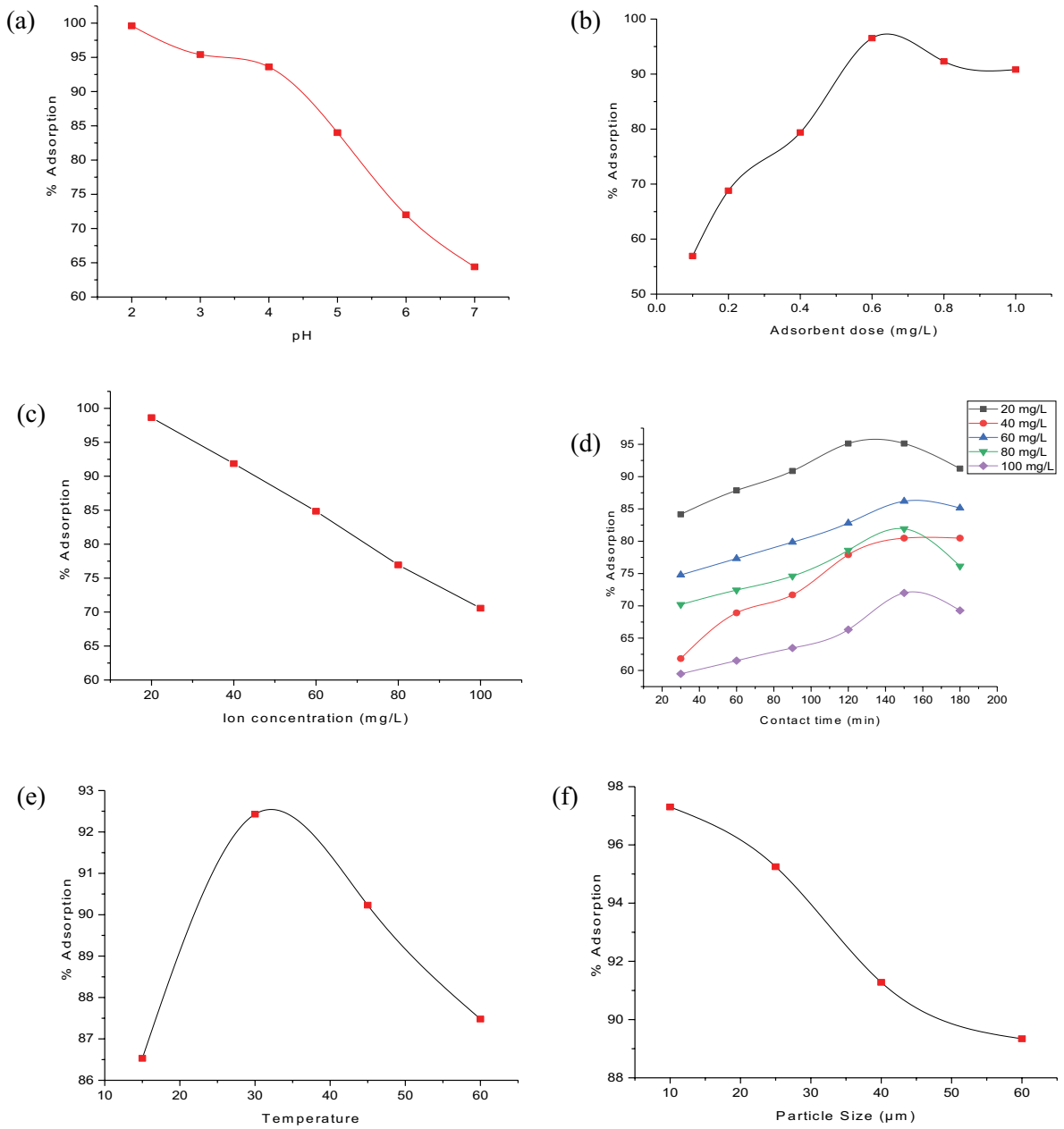

Fig. 5. Impact of adsorption efficiency by altering the characteristics of (a) pH, (b) biosorbent dose, (c) ion concentration, (d) time of reaction, (e) temperature and (f) size of *Ziziphus jujube* biosorbent.

particles. Fig. 5c represents the impact of metal ion uptake by adjusting the chromium concentration as 20, 40, 60, 80 and 100 mg/L. Taking the optimum pH and biochar dose the impacts were analyzed and discussed up to the constant attainment rate. The impact at 30°C was examined within 60 min of contact time and is depicted in Fig. 5c. In lower concentrations, the adsorbent's effectiveness of chromium ion absorption was quick, and 98.73% of chromium ions were removed from the synthetic solution in 20 mg/L. Due to significant wander walls forces, the availability of active sites in the synthetic solution was high at lower concentrations and rapidly absorbed by the adsorbent. When the concentration of metal ion-containing solution is high and the adsorbent has a low number of active sites, the quantity of pollutant uptake is reduced [24]. With an increase in metal ion concentration, the adsorption process approached saturation, and there was no change in adsorption efficiency after the saturation point. As a result, in batch adsorption investigations, the highest adsorption efficiency was reached at lower concentrations.

3.8. Impact of contact time

Fig. 5d depicts the effect of chromium ion adsorption on the contact duration between activated charcoal biosorbent and synthetic solution ranging from 30 to 180 min at

concentrations ranging from 20 to 100 mg/L. Similar to previous experiments, the contact time was adjusted and optimum biochar concentration of 0.6 g/L and pH of 2.0 obtained from the batch study was taken in this experimental work. When the adsorption process begins, the availability of active sites is greater, and it fills up quickly with contaminants. Later, the active site availability is extremely low, reducing pollutant adsorption from aqueous solutions [25]. After 90 min of contact time, the saturation point produced a rapid reduction in metal ion uptake by the activated biochar. As a result, the greatest quantity of pollutant adsorption occurred at the beginning of the adsorption phase.

3.9. Impact of temperature in metal ion adsorption

The industrial effluent's temperature is not a constant one and it may affect the efficiency of adsorption process. In this study, after determining the optimal values of pH, biochar dose, ion concentration, and reaction time from the above discussions, the impact of varying temperature of metal ion uptake was analyzed in the range of 15°C–60°C. Chromium adsorption increases with increasing temperature up to 30°C, and increasing temperature further inhibits metal ion absorption. The decrease in adsorption effectiveness with increasing temperature was caused by an increase in the rate of desorption in the adsorption process. Fig. 5e shows the effect of adsorption by varying the temperature of metal ion containing solutions.

3.10. Impact of particle size change in adsorption

The average particle size of the adsorbent material was obtained in BET analysis, and those particles were used for the adsorption process. To check the impact of particle size in the adsorption process, different sizes of particles (10, 25, 40 and 56 μm) were used in batch mode. Fig. 5f shows the adsorption efficiency changes by varying the adsorbent material's particle size. The efficiency of adsorption was decided based on the availability of surface area. The particle size is small; it has a very large surface area [26]. According to the graph, a 10μm particle provided a high efficiency of 97.27%, and increasing particle size steadily reduces adsorption efficiency. Also, the active site is less in smaller particle size, which can easily bind the adsorbent particles without surface contact. Due to this reason, the efficiency of adsorption was high in smaller particle sizes.

3.11. Adsorption isotherm al studies

3.11.1. Langmuir isotherm

Fig. 6a shows Langmuir isotherm linear plots (C_e/q_e against C_e) used to investigate chromium ion absorption and follow-up by monolayer or multilayer methods. The values of adsorption capacity and intensity were obtained from the linear plots of this study, and they were in good agreement with the standard values. Table 3 shows the computed parameters and their values for the Langmuir isotherm model. The separation parameter derived from the

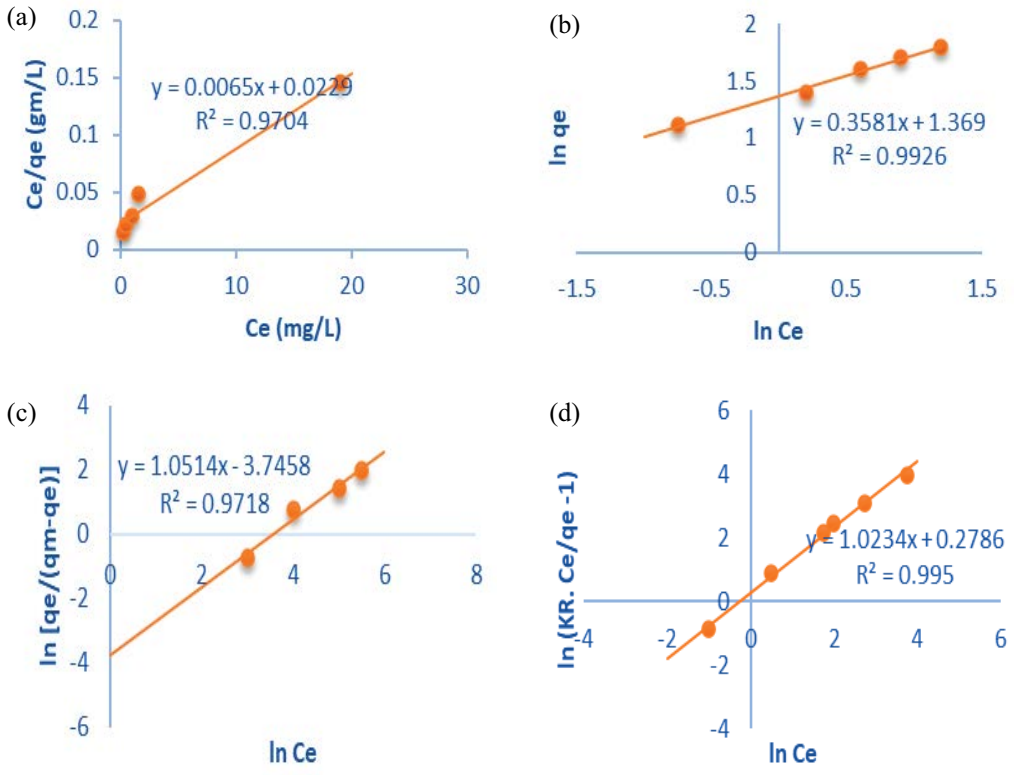

Fig. 6. (a) Langmuir, (b) Freundlich, (c) Sips and (d) Redlich–Peterson isotherm models for the adsorption of chromium ions using *Ziziphus jujube* biosorbent.

plot is 0.0034 between 0 and 1, confirming the adsorption follow-up operation. The regression coefficients (R^2) are more than 0.95, showing that the Langmuir isotherm model is applicable. As a result, the chromium ion absorption by the *Ziziphus jujube* biochar adsorbent is a homogenous monolayer process [27].

3.11.2. Freundlich study

The constant temperature distribution and heterogeneous nature of adsorption process has been evaluated by Freundlich isotherm studies. Fig. 6b shows the linear plots of Freundlich isothermal studies, and the constants of isothermal studies were evaluated and represented in Table 3. The value of adsorption capacity was 3.125 which falls between 0 to 1 shows the applicability of Freundlich isotherm study and Table 3 represents the constants of this model. In addition, the regression coefficient (R^2) is larger than 0.95, showing that the Freundlich isotherm model is suitable. As a result, the chromium absorption by *Ziziphus jujube* charcoal adsorbent is similarly heterogeneous, with a multilayer process [28].

3.11.3. Sips isotherm study

The chromium ion absorption by *Ziziphus jujube* charcoal adsorbent follows either Langmuir and Freundlich investigations, and adsorption occurs in both homogeneous and heterogeneous environments. As a result, in adsorption research, fitting the adsorption process is increasingly crucial [29]. The Sips isotherm models were fitted using the linear plots from the investigation, as shown in Fig. 6c. The process follows either the Langmuir or Freundlich fit, depending on the heterogeneity factor (n) number. If n is less than one, the procedure follows Freundlich fitting; if n is greater than one, the process follows Langmuir fitting. The Freundlich isotherm fitting of the chromium adsorption process by *Ziziphus jujube* biochar adsorbent resulted in an n value of 2.621, which is greater than 1, and a high regression value was obtained.

Table 3
Constants of isotherm models obtained from linear plots

Isotherm type	Constants	Values
Langmuir	q_{max}	10.283
	K_L	0.381
	R^2	0.9704
Freundlich	K_f	2.831
	n	2.621
	R^2	0.992
Redlich–Peterson	K_{RP}	12.912
	α_{RP}	0.364
	β_{RP}	1.183
	R^2	0.995
Sips	K_s	11.374
	β_s	1.437
	a_S	0.502
	R^2	0.971

3.11.4. Redlich–Peterson study

Redlich–Peterson study, commonly known as the three-parameter model, is used to identify the adsorption performance in clear way [30]. The Langmuir and Freundlich isotherms have just two undetermined values. On the other hand, the Redlich–Peterson isotherm has three undetermined variables that produce the precise values of the adsorption constants. The constants of Redlich–Peterson isothermal model were obtained from the linear plots are shown in Fig. 6d and the values are listed in Table 3. The constants of Redlich–Peterson model plot are shown in Table 3, and the regression value (R^2) was determined to be high (>0.95). The values of b_R have been utilized to match the adsorption process, either Langmuir or Freundlich isotherm. If b_R = 0, the adsorption process uses the Freundlich fitting approach, and if b_R = 1, the chromium absorption by *Ziziphus jujube* biochar uses the Langmuir fitting method.

3.12. Kinetic studies

3.12.1. Pseudo-first-order studies

Fig. 7a shows the linear plots of ($q_e - q$) vs. t used to investigate the kinetics of chromium ion adsorption by *Ziziphus jujube* biochar seeds adsorbent. Table 4 represents the values of pseudo-first-order kinetic model obtained from each plot in various concentrations of 25, 50, 75, 100, 125 and 150 mg/L. The table displays the plots' kinetic values (k) and regression coefficients (R^2), both of which were found to be acceptable and consistent with the adsorption process. Regression value on the linear plot is more than 0.95, demonstrating the model's relevance to chromium adsorption. In addition, based on the regression indicator, the adsorption process reached an equilibrium level.

3.12.2. Pseudo-second-order studies

Similar to the first order studies, the earlier stage ion concentration was adjusted as 25, 50, 75, 100, 125 and 150 mg/L and the constants were obtained in each linear plots of this study. Table 4 shows the constants obtained from the linear plots of the second-order kinetic model, which were calculated from this study, as illustrated in Fig. 7b. The q_e values derived using linear equations were almost identical to the q_e values derived through experimental analysis. The second-order studies also match well with the adsorption process based on the plot values, and it demonstrates the adsorption saturation point within the limiting behavior [31].

3.12.3. Elovich kinetics

Using Elovich kinetic experiments, the nature of the heterogeneous adsorption process under extreme conditions was examined. Fig. 7c depicts a linear plot of q_t vs ln(t), and the slope deflection values were collected and utilised to calculate the kinetic constants of a and b. Table 4 lists the various Elovich kinetic plot constants, and the regression value was relatively small. Based on the results of the regression investigations, this model does not correspond to the chromium adsorption process by *Ziziphus jujube* adsorbent. Referring to the first order studies, heterogeneous active sites are abundant, and the Elovich kinetic model does not

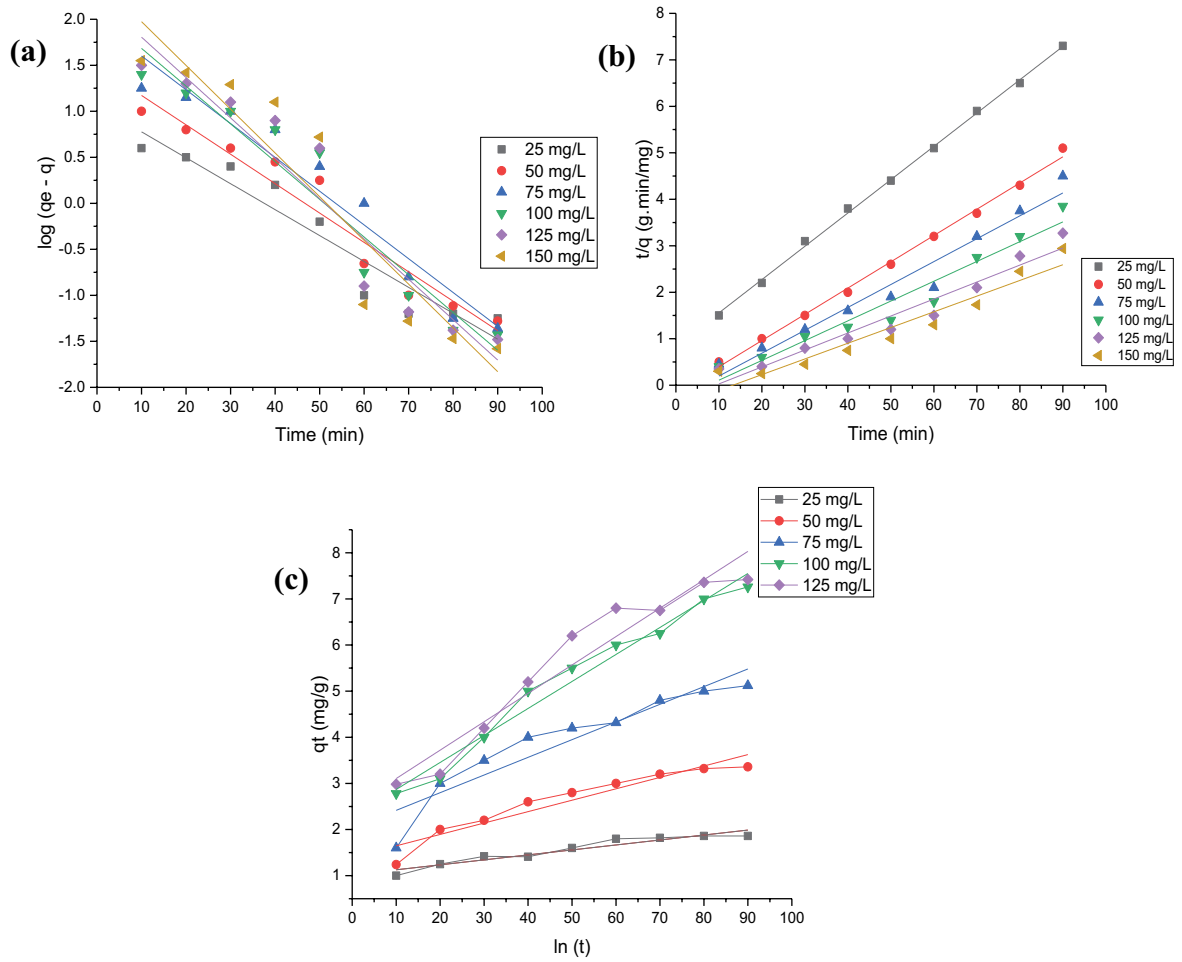

Fig. 7. Adsorption kinetics for metal ion removal using biochar by (a) pseudo-first-order, (b) pseudo-second-order and (c) Elovich studies.

Table 4
Chromium adsorption kinetic constants using *Ziziphus jujube* biosorbent

Conc. (mg/L)	Pseudo-first-order			Pseudo-second-order				Elovich		
	K (min^{-1})	q_e (mg/g)	R^2	$K \times 10^{-3}$ (g/mg·min)	q_e (mg/g)	h (mg/g·min)	R^2	a (mg/g·min)	b (g/mg)	R^2
20	0.041	3.21	0.97	18.41	2.13	0.15	0.97	0.413	1.72	0.93
40	0.059	7.04	0.95	15.38	5.48	0.17	0.95	0.854	0.95	0.92
60	0.072	10.23	0.98	10.53	8.64	0.24	0.97	0.983	0.64	0.94
80	0.063	13.82	0.97	6.49	10.84	0.27	0.96	0.942	0.41	0.92
100	0.051	17.38	0.97	2.18	13.53	0.34	0.97	0.889	0.27	0.93

anticipate this [32]. As a result, the kinetic model did not suit the chromium adsorption process.

3.13. Thermodynamic studies

The synthetic solution's chromium ion concentration was adjusted to range between 20 and 100 mg/L, and thermodynamic experiments were run to evaluate the adsorption process's thermodynamic behavior. Fig. 8 depicts thermodynamic graphs of the chromium ion adsorption process at 15°C, 30°C, 45°C, and 60°C, respectively. Taking the slope and deflection values from the thermodynamic plots the thermodynamic parameters (H_o and S_o) and its values were obtained. The Gibbs free energy (G_o) was measured at various temperatures; the results are shown in Table 5. Because of its spontaneous character, the Gibbs energy values are positive with negative enthalpy values, confirming that the adsorption process employing *Ziziphus jujube* biochar follows an endothermic reaction [33]. Furthermore, the entropy values are positive, supporting the liquid and

Table 5
Thermodynamic parameters of metal ion adsorption in various temperature level

Conc. of Cr^{6+} ions	Enthalpy (kJ/mol)	Entropy (J/mol)	Gibbs energy (kJ/mol)			
			15°C	30°C	45°C	60°C
20	82.384	162.394	–16.239	–12.673	–10.245	–8.642
40	42.942	80.283	–12.453	–9.236	–8.542	–6.585
60	19.943	41.532	–9.832	–5.215	–4.893	–4.028
80	12.643	29.658	–5.281	–4.639	–3.532	–2.984
100	8.382	20.391	–4.982	–3.482	–2.184	–1.845

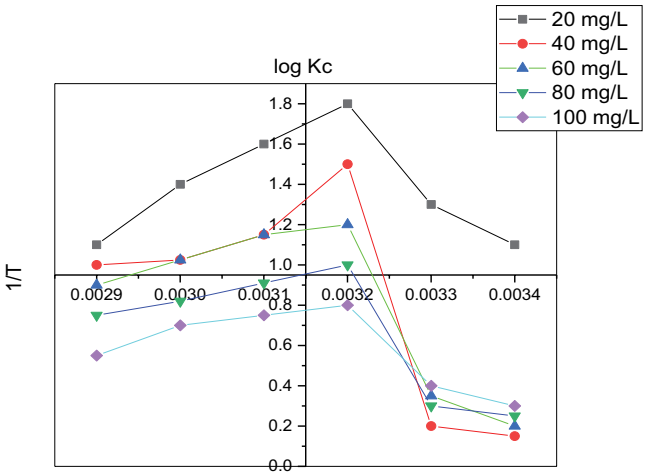

Fig. 8. Chromium adsorption thermodynamic plot using *Ziziphus jujube* biochar seeds powder.

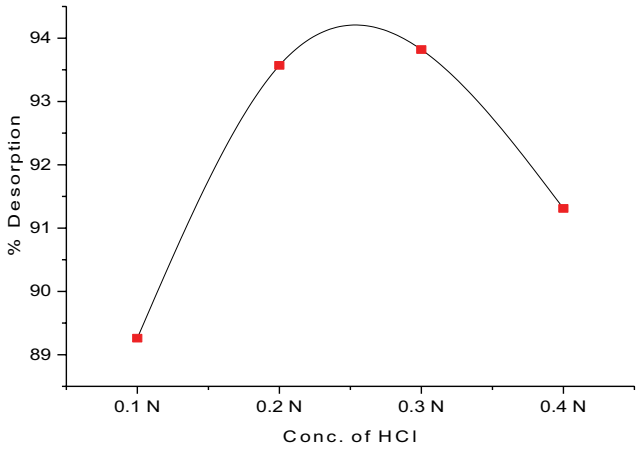

Fig. 9. Desorption curve of chromium ion uptake from the spent adsorbent.

solids uncertainty of chromium ion absorption utilizing *Ziziphus jujube* biochar material.

3.14. Desorption studies

Concentrated hydrochloric acid (0.1 to 0.4 N) was used in this study. The desorption tests were conducted to reuse the adsorbent materials and metal ions. The adsorbed materials were first treated with strong hydrochloric acid (0.1 N), which recovered 85.67% of the chromium ions from the solution. When the concentration was raised to 0.3 N, about 93.47% of the chromium ions were recovered from the adsorbed solutions. Fig. 9 shows that increasing the concentration reduces the quantity of metal ion recovery. Metal ion recovery decreased as hydrochloric acid concentration increased due to a decrease in active site availability. The metal ion recovery from the spent adsorbent was reduced due to the large volume of ions in the higher concentrations. As a result, in chromium adsorption investigations utilizing activated *Ziziphus jujube* biochar seeds powder, the highest quantity of wasted adsorbent was recovered by adding 0.3 N of hydrochloric acid.

4. Conclusion

Activated *Ziziphus jujube* biochar seeds were used in batch adsorption investigations of chromium ion absorption from synthetic solution. With pH range of 2.0, biosorbent dose of 0.6 g/L, and ion concentration of 20 mg/L, the chemically prepared activated carbon biosorbent adsorbs 99.27% of chromium ions in 90 min. Langmuir, Freundlich, Sips, and Redlich–Peterson isotherm studies match well with the adsorption process, and it is recommended that both monolayer and multilayer adsorption be followed. The pseudo-first and second-order kinetics suggest the heterogeneous nature and its applicability of metal ion uptake process by the adsorbent. Thermodynamic investigations were carried out to evaluate the endothermic behavior of the adsorption process under various temperatures and concentrations. The adsorption investigations show the adsorbent's capacity to remove chromium metal ions from aqueous solutions under regulated conditions.

Conflict of interest

The authors declare no conflict of interest.

Acknowledgement

The authors extend their appreciation to the Researchers Supporting Project number (RSP2023R396), King Saud University, Riyadh, Saudi Arabia.

References

[1] A.K. Priya, V. Yogeshwaran, S. Rajendran, T.K.A. Hoang, M. Soto-Moscoso, A.A. Ghfar, C. Bathula, Investigation of

mechanism of heavy metals (Cr^{6+}, Pb^{2+} & Zn^{2+}) adsorption from aqueous medium using rice husk ash: kinetic and thermodynamic approach, Chemosphere, 286 (2022) 131796, doi: 10.1016/j.chemosphere.2021.131796.
[2] A. Pholosi, E.B. Naidoo, A.E. Ofomaja, Intraparticle diffusion of Cr(VI) through biomass and magnetite coated biomass: A comparative kinetic and diffusion study, S. Afr. J. Chem. Eng., 32 (2020) 39–55.
[3] A. Eleryan, U.O. Aigbe, K.E. Ukhurebor, R.B. Onyancha, T.M. Eldeeb, M.A. El-Nemr, M.A. Hassaan, S. Ragab, O.A. Osibote, H.S. Kusuma, H. Darmokoesoemo, A. El Nemr, Copper(II) ion removal by chemically and physically modified sawdust biochar, Biomass Convers. Biorefin., 1 (2022) 1–38.
[4] A.K. Dey, A. Dey, R. Goswami, Adsorption characteristics of methyl red dye by Na_2CO_3-treated jute fibre using multi-criteria decision-making approach, Appl. Water Sci., 12 (2022) 1–22.
[5] S.M. Batagarawa, A.K. Ajibola, Comparative evaluation for the adsorption of toxic heavy metals on to millet, corn and rice husks as adsorbents, J. Anal. Pharm. Res., 8 (2019) 119–125.
[6] J. Bayuo, K.B. Pelig-Ba, M.A. Abukari, Adsorptive removal of chromium(VI) from aqueous solution unto groundnut shell, Appl. Water Sci., 9 (2019) 1–11.
[7] B.N. Pham, J.K. Kang, C.G. Lee, S.J. Park, Removal of heavy metals (Cd^{2+}, Cu^{2+}, Ni^{2+}, Pb^{2+}) from aqueous solution using *Hizikia fusiformis* as an algae-based bioadsorbent, Appl. Sci., 11 (2021) 8604, doi: 10.3390/app11188604.
[8] C. Wang, X. Wang, N. Li, J. Tao, B. Yan, X. Cui, G. Chen, Adsorption of lead from aqueous solution by biochar: a review, Clean Technol., 4 (2022) 629–652.
[9] D.A. Yaseen, M. Scholz, Textile dye wastewater characteristics and constituents of synthetic effluents: a critical review, Int. J. Environ. Sci. Technol., 16 (2019) 1193–1226.
[10] J. Singh, N. Dhiman, N.K. Sharma, Effect of Fe(II) on the adsorption of Mn(II) from aqueous solution using esterified saw dust: equilibrium and thermodynamic studies, Indian Chem. Eng., 60 (2017) 255–268.
[11] J. Hong, J. Xie, S. Mirshahghassemi, J. Lead, Metal (Cd, Cr, Ni, Pb) removal from environmentally relevant waters using polyvinylpyrrolidone-coated magnetite nanoparticles, RSC Adv., 10 (2020) 3266–3276.
[12] J.B. Dulla, M.R. Tamana, S. Boddu, K. Pulipati, K. Srirama, Biosorption of copper(II) onto spent biomass of *Gelidiella acerosa* (brown marine algae): optimization and kinetic studies, Appl. Water Sci., 10 (2020) 1–10.
[13] M. Feszterová, L. Porubcová, A. Tirpáková, The monitoring of selected heavy metals content and bioavailability in the soil-plant system and its impact on sustainability in agribusiness food chains, Sustainability, 13 (2021) 7021, doi: 10.3390/su13137021.
[14] M. Benjelloun, Y. Miyah, G. Akdemir Evrendilek, F. Zerrouq, S. Lairini, Recent advances in adsorption kinetic models: their application to dye types, Arabian J. Chem., 14 (2021) 103031, doi: 10.1016/j.arabjc.2021.103031.
[15] N.S. Langeroodi, Z. Farhadravesh, A.D. Khalaji, Optimization of adsorption parameters for Fe(III) ions removal from aqueous solutions by transition metal oxide nanocomposite, Green Chem. Lett. Rev., 11 (2018) 404–413.
[16] N. Fakhar, S. Ayoub Khan, W. Ahmad Siddiqi, T. Alam Khan, *Ziziphus jujube* waste-derived biomass as cost-effective adsorbent for the sequestration of Cd^{2+} from aqueous solution: isotherm and kinetics studies, Environ. Nanotechnol. Monit. Manage., 16 (2021) 100570, doi: 10.1016/j.enmm.2021.100570.
[17] N.M. Malima, S.J. Owonubi, E.H. Lugwisha, A.S. Mwakaboko, Thermodynamic, isothermal and kinetic studies of heavy metals adsorption by chemically modified Tanzanian Malangali kaolin clay, Int. J. Environ. Sci. Technol., 18 (2021) 3153–3168.
[18] P. Phuengphai, T. Singjanusong, N. Kheangkhun, A. Wattanakornsiri, Removal of copper(II) from aqueous solution using chemically modified fruit peels as efficient low-cost biosorbents, Water Sci. Eng., 14 (2021) 286–294.
[19] Pragati, S. Singh Trivedia, L. Pandey, Removal of zinc from synthetic wastewater by saw dust as an adsorbent, IJISET-Int. J. Innov. Sci. Eng. Technol., 2 (2015) 120–127.
[20] R. Labied, O. Benturki, A.Y. Eddine Hamitouche, A. Donnot, Adsorption of hexavalent chromium by activated carbon obtained from a waste lignocellulosic material (*Ziziphus jujuba* cores): kinetic, equilibrium, and thermodynamic study, Adsorpt. Sci. Technol., 36 (2018) 1066–1099.
[21] R.A. Fideles, F.S. Teodoro, A.L.P. Xavier, O.F.H. Adarme, L.F. Gil, L.V.A. Gurgel, Trimellitated sugarcane bagasse: a versatile adsorbent for removal of cationic dyes from aqueous solution. Part II: Batch and continuous adsorption in a bicomponent system, J. Colloid Interface Sci., 552 (2019) 752–763.
[22] R. Chakraborty, A. Asthana, A.K. Singh, B. Jain, A.B.H. Susan, Adsorption of heavy metal ions by various low-cost adsorbents: a review, 102 (2020) 342–379.
[23] S. Candamano, A. Policicchio, G. Conte, R. Abarca, C. Algieri, S. Chakraborty, S. Curcio, V. Calabrò, F. Crea, R.G. Agostino, Preparation of foamed and unfoamed geopolymer/NaX zeolite/activated carbon composites for CO_2 adsorption, J. Cleaner Prod., 330 (2022) 129843, doi: 10.1016/j.jclepro.2021.129843.
[24] T.G. Walmsley, P.S. Varbanov, R. Su, J.J. Klemeš, S. Sirusbakht, L. Vafajoo, S. Soltani, S. Habibi, Sawdust biosorption of chromium(VI) ions from aqueous solutions, Chem. Eng. Trans., 70 (2018) 1147–1152.
[25] Saruchi, V. Kumar, Adsorption kinetics and isotherms for the removal of rhodamine B dye and Pb^{+2} ions from aqueous solutions by a hybrid ion-exchanger, Arabian J. Chem., 12 (2019) 316–329.
[26] S. Velusamy, A. Roy, S. Sundaram, T. Kumar Mallick, A review on heavy metal ions and containing dyes removal through graphene oxide-based adsorption strategies for textile wastewater treatment, Chem. Rec., 21 (2021) 1570–1610.
[27] T.G. Ambaye, M. Vaccari, E.D. van Hullebusch, A. Amrane, S. Rtimi, Mechanisms and adsorption capacities of biochar for the removal of organic and inorganic pollutants from industrial wastewater, Int. J. Environ. Sci. Technol., 18 (2020) 3273–3294.
[28] T.A. Khan, Md. Nouman, D. Dua, S.A. Khan, S.S. Alharthi, Adsorptive scavenging of cationic dyes from aquatic phase by H_3PO_4 activated Indian jujube (*Ziziphus mauritiana*) seeds based activated carbon: isotherm, kinetics, and thermodynamic study, J. Saudi Chem. Soc., 26 (2022) 101417, doi: 10.1016/j.jscs.2021.101417.
[29] U.A. Edet, A.O. Ifelebuegu, Kinetics, isotherms, and thermodynamic modeling of the adsorption of phosphates from model wastewater using recycled brick waste, Processes, 8 (2020) 665, doi: 10.3390/pr8060665.
[30] V. Yogeshwaran, A.K. Priya, Experimental studies on the removal of heavy metal ion concentration using sugarcane bagasse in batch adsorption process, Desal. Water Treat., 224 (2021) 256–272.
[31] V. Kromah, G. Zhang, Aqueous adsorption of heavy metals on metal sulfide nanomaterials: synthesis and application, Water, 13 (2021) 1843, doi: 10.3390/w13131843.
[32] W. Kaminski, E. Tomczak, P. Tosik, Kinetics of azo dyes sorption onto low-cost sorbents, Desal. Water Treat., 55 (2014) 2675–2679.
[33] Y. Venkatraman, A.K. Priya, Removal of heavy metal ion concentrations from the wastewater using tobacco leaves coated with iron oxide nanoparticles, Int. J. Environ. Sci. Technol., 19 (2022) 2721–2736.